EUROPEAN ORGANIZATION FOR NUCLEAR RESEARCH (CERN)

CERN-PH-EP-2013-141
LHCb-PAPER-2013-033
August 5, 2013

Measurement of the flavour-specific *CP*-violating asymmetry $a^s_{\rm sl}$ in B^0_s decays

The LHCb collaboration[†]

Abstract

The *CP*-violating asymmetry $a^{\rm s}_{\rm sl}$ is studied using semileptonic decays of B^0_s and $\overline{B}{}^0_s$ mesons produced in pp collisions at a centre-of-mass energy of 7 TeV at the LHC, exploiting a data sample corresponding to an integrated luminosity of $1.0\,{\rm fb}^{-1}$. The reconstructed final states are $D^\pm_s\mu^\mp$, with the $D^\pm_s$ particle decaying in the $\phi\pi^\pm$ mode. The $D^\pm_s\mu^\mp$ yields are summed over $\overline{B}{}^0_s$ and B^0_s initial states, and integrated with respect to decay time. Data-driven methods are used to measure efficiency ratios. We obtain $a^{\rm s}_{\rm sl} = (-0.06 \pm 0.50 \pm 0.36)\%$, where the first uncertainty is statistical and the second systematic.

Submitted to Phys. Lett. B

[†]Authors are listed on the following pages.

LHCb collaboration

R. Aaij[40], B. Adeva[36], M. Adinolfi[45], C. Adrover[6], A. Affolder[51], Z. Ajaltouni[5], J. Albrecht[9], F. Alessio[37], M. Alexander[50], S. Ali[40], G. Alkhazov[29], P. Alvarez Cartelle[36], A.A. Alves Jr[24,37], S. Amato[2], S. Amerio[21], Y. Amhis[7], L. Anderlini[17,f], J. Anderson[39], R. Andreassen[56], J.E. Andrews[57], R.B. Appleby[53], O. Aquines Gutierrez[10], F. Archilli[18], A. Artamonov[34], M. Artuso[58], E. Aslanides[6], G. Auriemma[24,m], M. Baalouch[5], S. Bachmann[11], J.J. Back[47], C. Baesso[59], V. Balagura[30], W. Baldini[16], R.J. Barlow[53], C. Barschel[37], S. Barsuk[7], W. Barter[46], Th. Bauer[40], A. Bay[38], J. Beddow[50], F. Bedeschi[22], I. Bediaga[1], S. Belogurov[30], K. Belous[34], I. Belyaev[30], E. Ben-Haim[8], G. Bencivenni[18], S. Benson[49], J. Benton[45], A. Berezhnoy[31], R. Bernet[39], M.-O. Bettler[46], M. van Beuzekom[40], A. Bien[11], S. Bifani[44], T. Bird[53], A. Bizzeti[17,h], P.M. Bjørnstad[53], T. Blake[37], F. Blanc[38], J. Blouw[11], S. Blusk[58], V. Bocci[24], A. Bondar[33], N. Bondar[29], W. Bonivento[15], S. Borghi[53], A. Borgia[58], T.J.V. Bowcock[51], E. Bowen[39], C. Bozzi[16], T. Brambach[9], J. van den Brand[41], J. Bressieux[38], D. Brett[53], M. Britsch[10], T. Britton[58], N.H. Brook[45], H. Brown[51], I. Burducea[28], A. Bursche[39], G. Busetto[21,q], J. Buytaert[37], S. Cadeddu[15], O. Callot[7], M. Calvi[20,j], M. Calvo Gomez[35,n], A. Camboni[35], P. Campana[18,37], D. Campora Perez[37], A. Carbone[14,c], G. Carboni[23,k], R. Cardinale[19,i], A. Cardini[15], H. Carranza-Mejia[49], L. Carson[52], K. Carvalho Akiba[2], G. Casse[51], L. Castillo Garcia[37], M. Cattaneo[37], Ch. Cauet[9], R. Cenci[57], M. Charles[54], Ph. Charpentier[37], P. Chen[3,38], N. Chiapolini[39], M. Chrzaszcz[25], K. Ciba[37], X. Cid Vidal[37], G. Ciezarek[52], P.E.L. Clarke[49], M. Clemencic[37], H.V. Cliff[46], J. Closier[37], C. Coca[28], V. Coco[40], J. Cogan[6], E. Cogneras[5], P. Collins[37], A. Comerma-Montells[35], A. Contu[15,37], A. Cook[45], M. Coombes[45], S. Coquereau[8], G. Corti[37], B. Couturier[37], G.A. Cowan[49], D.C. Craik[47], S. Cunliffe[52], R. Currie[49], C. D'Ambrosio[37], P. David[8], P.N.Y. David[40], A. Davis[56], I. De Bonis[4], K. De Bruyn[40], S. De Capua[53], M. De Cian[11], J.M. De Miranda[1], L. De Paula[2], W. De Silva[56], P. De Simone[18], D. Decamp[4], M. Deckenhoff[9], L. Del Buono[8], N. Déléage[4], D. Derkach[54], O. Deschamps[5], F. Dettori[41], A. Di Canto[11], H. Dijkstra[37], M. Dogaru[28], S. Donleavy[51], F. Dordei[11], A. Dosil Suárez[36], D. Dossett[47], A. Dovbnya[42], F. Dupertuis[38], P. Durante[37], R. Dzhelyadin[34], A. Dziurda[25], A. Dzyuba[29], S. Easo[48], U. Egede[52], V. Egorychev[30], S. Eidelman[33], D. van Eijk[40], S. Eisenhardt[49], U. Eitschberger[9], R. Ekelhof[9], L. Eklund[50,37], I. El Rifai[5], Ch. Elsasser[39], A. Falabella[14,e], C. Färber[11], G. Fardell[49], C. Farinelli[40], S. Farry[51], D. Ferguson[49], V. Fernandez Albor[36], F. Ferreira Rodrigues[1], M. Ferro-Luzzi[37], S. Filippov[32], M. Fiore[16], C. Fitzpatrick[37], M. Fontana[10], F. Fontanelli[19,i], R. Forty[37], O. Francisco[2], M. Frank[37], C. Frei[37], M. Frosini[17,f], S. Furcas[20], E. Furfaro[23,k], A. Gallas Torreira[36], D. Galli[14,c], M. Gandelman[2], P. Gandini[58], Y. Gao[3], J. Garofoli[58], P. Garosi[53], J. Garra Tico[46], L. Garrido[35], C. Gaspar[37], R. Gauld[54], E. Gersabeck[11], M. Gersabeck[53], T. Gershon[47,37], Ph. Ghez[4], V. Gibson[46], L. Giubega[28], V.V. Gligorov[37], C. Göbel[59],

D. Golubkov[30], A. Golutvin[52,30,37], A. Gomes[2], P. Gorbounov[30,37], H. Gordon[37], C. Gotti[20], M. Grabalosa Gándara[5], R. Graciani Diaz[35], L.A. Granado Cardoso[37], E. Graugés[35], G. Graziani[17], A. Grecu[28], E. Greening[54], S. Gregson[46], P. Griffith[44], O. Grünberg[60], B. Gui[58], E. Gushchin[32], Yu. Guz[34,37], T. Gys[37], C. Hadjivasiliou[58], G. Haefeli[38], C. Haen[37], S.C. Haines[46], S. Hall[52], B. Hamilton[57], T. Hampson[45], S. Hansmann-Menzemer[11], N. Harnew[54], S.T. Harnew[45], J. Harrison[53], T. Hartmann[60], J. He[37], T. Head[37], V. Heijne[40], K. Hennessy[51], P. Henrard[5], J.A. Hernando Morata[36], E. van Herwijnen[37], M. Hess[60], A. Hicheur[1], E. Hicks[51], D. Hill[54], M. Hoballah[5], C. Hombach[53], P. Hopchev[4], W. Hulsbergen[40], P. Hunt[54], T. Huse[51], N. Hussain[54], D. Hutchcroft[51], D. Hynds[50], V. Iakovenko[43], M. Idzik[26], P. Ilten[12], R. Jacobsson[37], A. Jaeger[11], E. Jans[40], P. Jaton[38], A. Jawahery[57], F. Jing[3], M. John[54], D. Johnson[54], C.R. Jones[46], C. Joram[37], B. Jost[37], M. Kaballo[9], S. Kandybei[42], W. Kanso[6], M. Karacson[37], T.M. Karbach[37], I.R. Kenyon[44], T. Ketel[41], A. Keune[38], B. Khanji[20], O. Kochebina[7], I. Komarov[38], R.F. Koopman[41], P. Koppenburg[40], M. Korolev[31], A. Kozlinskiy[40], L. Kravchuk[32], K. Kreplin[11], M. Kreps[47], G. Krocker[11], P. Krokovny[33], F. Kruse[9], M. Kucharczyk[20,25,j], V. Kudryavtsev[33], T. Kvaratskheliya[30,37], V.N. La Thi[38], D. Lacarrere[37], G. Lafferty[53], A. Lai[15], D. Lambert[49], R.W. Lambert[41], E. Lanciotti[37], G. Lanfranchi[18], C. Langenbruch[37], T. Latham[47], C. Lazzeroni[44], R. Le Gac[6], J. van Leerdam[40], J.-P. Lees[4], R. Lefèvre[5], A. Leflat[31], J. Lefrançois[7], S. Leo[22], O. Leroy[6], T. Lesiak[25], B. Leverington[11], Y. Li[3], L. Li Gioi[5], M. Liles[51], R. Lindner[37], C. Linn[11], B. Liu[3], G. Liu[37], S. Lohn[37], I. Longstaff[50], J.H. Lopes[2], N. Lopez-March[38], H. Lu[3], D. Lucchesi[21,q], J. Luisier[38], H. Luo[49], F. Machefert[7], I.V. Machikhiliyan[4,30], F. Maciuc[28], O. Maev[29,37], S. Malde[54], G. Manca[15,d], G. Mancinelli[6], J. Maratas[5], U. Marconi[14], P. Marino[22,s], R. Märki[38], J. Marks[11], G. Martellotti[24], A. Martens[8], A. Martín Sánchez[7], M. Martinelli[40], D. Martinez Santos[41], D. Martins Tostes[2], A. Martynov[31], A. Massafferri[1], R. Matev[37], Z. Mathe[37], C. Matteuzzi[20], E. Maurice[6], A. Mazurov[16,32,37,e], J. McCarthy[44], A. McNab[53], R. McNulty[12], B. McSkelly[51], B. Meadows[56,54], F. Meier[9], M. Meissner[11], M. Merk[40], D.A. Milanes[8], M.-N. Minard[4], J. Molina Rodriguez[59], S. Monteil[5], D. Moran[53], P. Morawski[25], A. Mordà[6], M.J. Morello[22,s], R. Mountain[58], I. Mous[40], F. Muheim[49], K. Müller[39], R. Muresan[28], B. Muryn[26], B. Muster[38], P. Naik[45], T. Nakada[38], R. Nandakumar[48], I. Nasteva[1], M. Needham[49], S. Neubert[37], N. Neufeld[37], A.D. Nguyen[38], T.D. Nguyen[38], C. Nguyen-Mau[38,o], M. Nicol[7], V. Niess[5], R. Niet[9], N. Nikitin[31], T. Nikodem[11], A. Nomerotski[54], A. Novoselov[34], A. Oblakowska-Mucha[26], V. Obraztsov[34], S. Oggero[40], S. Ogilvy[50], O. Okhrimenko[43], R. Oldeman[15,d], M. Orlandea[28], J.M. Otalora Goicochea[2], P. Owen[52], A. Oyanguren[35], B.K. Pal[58], A. Palano[13,b], T. Palczewski[27], M. Palutan[18], J. Panman[37], A. Papanestis[48], M. Pappagallo[50], C. Parkes[53], C.J. Parkinson[52], G. Passaleva[17], G.D. Patel[51], M. Patel[52], G.N. Patrick[48],

C. Patrignani[19,i], C. Pavel-Nicorescu[28], A. Pazos Alvarez[36], A. Pellegrino[40], G. Penso[24,l], M. Pepe Altarelli[37], S. Perazzini[14,c], E. Perez Trigo[36], A. Pérez-Calero Yzquierdo[35], P. Perret[5], M. Perrin-Terrin[6], L. Pescatore[44], E. Pesen[61], K. Petridis[52], A. Petrolini[19,i], A. Phan[58], E. Picatoste Olloqui[35], B. Pietrzyk[4], T. Pilař[47], D. Pinci[24], S. Playfer[49], M. Plo Casasus[36], F. Polci[8], G. Polok[25], A. Poluektov[47,33], E. Polycarpo[2], A. Popov[34], D. Popov[10], B. Popovici[28], C. Potterat[35], A. Powell[54], J. Prisciandaro[38], A. Pritchard[51], C. Prouve[7], V. Pugatch[43], A. Puig Navarro[38], G. Punzi[22,r], W. Qian[4], J.H. Rademacker[45], B. Rakotomiaramanana[38], M.S. Rangel[2], I. Raniuk[42], N. Rauschmayr[37], G. Raven[41], S. Redford[54], M.M. Reid[47], A.C. dos Reis[1], S. Ricciardi[48], A. Richards[52], K. Rinnert[51], V. Rives Molina[35], D.A. Roa Romero[5], P. Robbe[7], D.A. Roberts[57], E. Rodrigues[53], P. Rodriguez Perez[36], S. Roiser[37], V. Romanovsky[34], A. Romero Vidal[36], J. Rouvinet[38], T. Ruf[37], F. Ruffini[22], H. Ruiz[35], P. Ruiz Valls[35], G. Sabatino[24,k], J.J. Saborido Silva[36], N. Sagidova[29], P. Sail[50], B. Saitta[15,d], V. Salustino Guimaraes[2], B. Sanmartin Sedes[36], M. Sannino[19,i], R. Santacesaria[24], C. Santamarina Rios[36], E. Santovetti[23,k], M. Sapunov[6], A. Sarti[18,l], C. Satriano[24,m], A. Satta[23], M. Savrie[16,e], D. Savrina[30,31], P. Schaack[52], M. Schiller[41], H. Schindler[37], M. Schlupp[9], M. Schmelling[10], B. Schmidt[37], O. Schneider[38], A. Schopper[37], M.-H. Schune[7], R. Schwemmer[37], B. Sciascia[18], A. Sciubba[24], M. Seco[36], A. Semennikov[30], K. Senderowska[26], I. Sepp[52], N. Serra[39], J. Serrano[6], P. Seyfert[11], M. Shapkin[34], I. Shapoval[16,42], P. Shatalov[30], Y. Shcheglov[29], T. Shears[51,37], L. Shekhtman[33], O. Shevchenko[42], V. Shevchenko[30], A. Shires[9], R. Silva Coutinho[47], M. Sirendi[46], N. Skidmore[45], T. Skwarnicki[58], N.A. Smith[51], E. Smith[54,48], J. Smith[46], M. Smith[53], M.D. Sokoloff[56], F.J.P. Soler[50], F. Soomro[18], D. Souza[45], B. Souza De Paula[2], B. Spaan[9], A. Sparkes[49], P. Spradlin[50], F. Stagni[37], S. Stahl[11], O. Steinkamp[39], S. Stevenson[54], S. Stoica[28], S. Stone[58], B. Storaci[39], M. Straticiuc[28], U. Straumann[39], V.K. Subbiah[37], L. Sun[56], S. Swientek[9], V. Syropoulos[41], M. Szczekowski[27], P. Szczypka[38,37], T. Szumlak[26], S. T'Jampens[4], M. Teklishyn[7], E. Teodorescu[28], F. Teubert[37], C. Thomas[54], E. Thomas[37], J. van Tilburg[11], V. Tisserand[4], M. Tobin[38], S. Tolk[41], D. Tonelli[37], S. Topp-Joergensen[54], N. Torr[54], E. Tournefier[4,52], S. Tourneur[38], M.T. Tran[38], M. Tresch[39], A. Tsaregorodtsev[6], P. Tsopelas[40], N. Tuning[40], M. Ubeda Garcia[37], A. Ukleja[27], D. Urner[53], A. Ustyuzhanin[52,p], U. Uwer[11], V. Vagnoni[14], G. Valenti[14], A. Vallier[7], M. Van Dijk[45], R. Vazquez Gomez[18], P. Vazquez Regueiro[36], C. Vázquez Sierra[36], S. Vecchi[16], J.J. Velthuis[45], M. Veltri[17,g], G. Veneziano[38], M. Vesterinen[37], B. Viaud[7], D. Vieira[2], X. Vilasis-Cardona[35,n], A. Vollhardt[39], D. Volyanskyy[10], D. Voong[45], A. Vorobyev[29], V. Vorobyev[33], C. Voß[60], H. Voss[10], R. Waldi[60], C. Wallace[47], R. Wallace[12], S. Wandernoth[11], J. Wang[58], D.R. Ward[46], N.K. Watson[44], A.D. Webber[53], D. Websdale[52], M. Whitehead[47], J. Wicht[37], J. Wiechczynski[25], D. Wiedner[11], L. Wiggers[40], G. Wilkinson[54], M.P. Williams[47,48], M. Williams[55], F.F. Wilson[48], J. Wimberley[57], J. Wishahi[9],

W. Wislicki[27], M. Witek[25], S.A. Wotton[46], S. Wright[46], S. Wu[3], K. Wyllie[37], Y. Xie[49,37], Z. Xing[58], Z. Yang[3], R. Young[49], X. Yuan[3], O. Yushchenko[34], M. Zangoli[14], M. Zavertyaev[10,a], F. Zhang[3], L. Zhang[58], W.C. Zhang[12], Y. Zhang[3], A. Zhelezov[11], A. Zhokhov[30], L. Zhong[3], A. Zvyagin[37].

[1] *Centro Brasileiro de Pesquisas Físicas (CBPF), Rio de Janeiro, Brazil*
[2] *Universidade Federal do Rio de Janeiro (UFRJ), Rio de Janeiro, Brazil*
[3] *Center for High Energy Physics, Tsinghua University, Beijing, China*
[4] *LAPP, Université de Savoie, CNRS/IN2P3, Annecy-Le-Vieux, France*
[5] *Clermont Université, Université Blaise Pascal, CNRS/IN2P3, LPC, Clermont-Ferrand, France*
[6] *CPPM, Aix-Marseille Université, CNRS/IN2P3, Marseille, France*
[7] *LAL, Université Paris-Sud, CNRS/IN2P3, Orsay, France*
[8] *LPNHE, Université Pierre et Marie Curie, Université Paris Diderot, CNRS/IN2P3, Paris, France*
[9] *Fakultät Physik, Technische Universität Dortmund, Dortmund, Germany*
[10] *Max-Planck-Institut für Kernphysik (MPIK), Heidelberg, Germany*
[11] *Physikalisches Institut, Ruprecht-Karls-Universität Heidelberg, Heidelberg, Germany*
[12] *School of Physics, University College Dublin, Dublin, Ireland*
[13] *Sezione INFN di Bari, Bari, Italy*
[14] *Sezione INFN di Bologna, Bologna, Italy*
[15] *Sezione INFN di Cagliari, Cagliari, Italy*
[16] *Sezione INFN di Ferrara, Ferrara, Italy*
[17] *Sezione INFN di Firenze, Firenze, Italy*
[18] *Laboratori Nazionali dell'INFN di Frascati, Frascati, Italy*
[19] *Sezione INFN di Genova, Genova, Italy*
[20] *Sezione INFN di Milano Bicocca, Milano, Italy*
[21] *Sezione INFN di Padova, Padova, Italy*
[22] *Sezione INFN di Pisa, Pisa, Italy*
[23] *Sezione INFN di Roma Tor Vergata, Roma, Italy*
[24] *Sezione INFN di Roma La Sapienza, Roma, Italy*
[25] *Henryk Niewodniczanski Institute of Nuclear Physics Polish Academy of Sciences, Kraków, Poland*
[26] *AGH - University of Science and Technology, Faculty of Physics and Applied Computer Science, Kraków, Poland*
[27] *National Center for Nuclear Research (NCBJ), Warsaw, Poland*
[28] *Horia Hulubei National Institute of Physics and Nuclear Engineering, Bucharest-Magurele, Romania*
[29] *Petersburg Nuclear Physics Institute (PNPI), Gatchina, Russia*
[30] *Institute of Theoretical and Experimental Physics (ITEP), Moscow, Russia*
[31] *Institute of Nuclear Physics, Moscow State University (SINP MSU), Moscow, Russia*
[32] *Institute for Nuclear Research of the Russian Academy of Sciences (INR RAN), Moscow, Russia*
[33] *Budker Institute of Nuclear Physics (SB RAS) and Novosibirsk State University, Novosibirsk, Russia*
[34] *Institute for High Energy Physics (IHEP), Protvino, Russia*
[35] *Universitat de Barcelona, Barcelona, Spain*
[36] *Universidad de Santiago de Compostela, Santiago de Compostela, Spain*
[37] *European Organization for Nuclear Research (CERN), Geneva, Switzerland*

[38] *Ecole Polytechnique Fédérale de Lausanne (EPFL), Lausanne, Switzerland*
[39] *Physik-Institut, Universität Zürich, Zürich, Switzerland*
[40] *Nikhef National Institute for Subatomic Physics, Amsterdam, The Netherlands*
[41] *Nikhef National Institute for Subatomic Physics and VU University Amsterdam, Amsterdam, The Netherlands*
[42] *NSC Kharkiv Institute of Physics and Technology (NSC KIPT), Kharkiv, Ukraine*
[43] *Institute for Nuclear Research of the National Academy of Sciences (KINR), Kyiv, Ukraine*
[44] *University of Birmingham, Birmingham, United Kingdom*
[45] *H.H. Wills Physics Laboratory, University of Bristol, Bristol, United Kingdom*
[46] *Cavendish Laboratory, University of Cambridge, Cambridge, United Kingdom*
[47] *Department of Physics, University of Warwick, Coventry, United Kingdom*
[48] *STFC Rutherford Appleton Laboratory, Didcot, United Kingdom*
[49] *School of Physics and Astronomy, University of Edinburgh, Edinburgh, United Kingdom*
[50] *School of Physics and Astronomy, University of Glasgow, Glasgow, United Kingdom*
[51] *Oliver Lodge Laboratory, University of Liverpool, Liverpool, United Kingdom*
[52] *Imperial College London, London, United Kingdom*
[53] *School of Physics and Astronomy, University of Manchester, Manchester, United Kingdom*
[54] *Department of Physics, University of Oxford, Oxford, United Kingdom*
[55] *Massachusetts Institute of Technology, Cambridge, MA, United States*
[56] *University of Cincinnati, Cincinnati, OH, United States*
[57] *University of Maryland, College Park, MD, United States*
[58] *Syracuse University, Syracuse, NY, United States*
[59] *Pontifícia Universidade Católica do Rio de Janeiro (PUC-Rio), Rio de Janeiro, Brazil, associated to* [2]
[60] *Institut für Physik, Universität Rostock, Rostock, Germany, associated to* [11]
[61] *Celal Bayar University, Manisa, Turkey, associated to* [37]

[a] *P.N. Lebedev Physical Institute, Russian Academy of Science (LPI RAS), Moscow, Russia*
[b] *Università di Bari, Bari, Italy*
[c] *Università di Bologna, Bologna, Italy*
[d] *Università di Cagliari, Cagliari, Italy*
[e] *Università di Ferrara, Ferrara, Italy*
[f] *Università di Firenze, Firenze, Italy*
[g] *Università di Urbino, Urbino, Italy*
[h] *Università di Modena e Reggio Emilia, Modena, Italy*
[i] *Università di Genova, Genova, Italy*
[j] *Università di Milano Bicocca, Milano, Italy*
[k] *Università di Roma Tor Vergata, Roma, Italy*
[l] *Università di Roma La Sapienza, Roma, Italy*
[m] *Università della Basilicata, Potenza, Italy*
[n] *LIFAELS, La Salle, Universitat Ramon Llull, Barcelona, Spain*
[o] *Hanoi University of Science, Hanoi, Viet Nam*
[p] *Institute of Physics and Technology, Moscow, Russia*
[q] *Università di Padova, Padova, Italy*
[r] *Università di Pisa, Pisa, Italy*

[s] *Scuola Normale Superiore, Pisa, Italy*

1 Introduction

The *CP* asymmetry in $B_s^0 - \overline{B}_s^0$ mixing is a sensitive probe of new physics. In the neutral B system (B^0 or B_s^0), the mixing of the flavour eigenstates (the neutral B and its antiparticle $\overline{B}$) is governed by a 2×2 complex effective Hamiltonian matrix [1]

$$\begin{pmatrix} M_{11} - \frac{i}{2}\Gamma_{11} & M_{12} - \frac{i}{2}\Gamma_{12} \\ M_{12}^* - \frac{i}{2}\Gamma_{12}^* & M_{22} - \frac{i}{2}\Gamma_{22} \end{pmatrix}, \tag{1}$$

which operates on the neutral B and $\overline{B}$ flavour eigenstates. The mass eigenstates have eigenvalues $M_{\rm H}$ and $M_{\rm L}$. Other measurable quantities are the mass difference ΔM, the width difference $\Delta\Gamma$, and the semileptonic (or flavour-specific) asymmetry $a_{\rm sl}$. These quantities are related to the off-diagonal matrix elements and the phase $\phi_{12} \equiv \arg\left(-M_{12}/\Gamma_{12}\right)$ by

$$\begin{aligned} \Delta M &\equiv M_{\rm H} - M_{\rm L} = 2|M_{12}|\left(1 - \frac{1}{8}\frac{|\Gamma_{12}|^2}{|M_{12}|^2}\sin^2\phi_{12} + ...\right), \\ \Delta\Gamma &\equiv \Gamma_{\rm L} - \Gamma_{\rm H} = 2|\Gamma_{12}|\cos\phi_{12}\left(1 + \frac{1}{8}\frac{|\Gamma_{12}|^2}{|M_{12}|^2}\sin^2\phi_{12} + ...\right), \\ a_{\rm sl} &\equiv \frac{\Gamma\left(\overline{B}(t) \to f\right) - \Gamma\left(B(t) \to \bar{f}\right)}{\Gamma\left(\overline{B}(t) \to f\right) + \Gamma\left(B(t) \to \bar{f}\right)} \simeq \frac{\Delta\Gamma}{\Delta M}\tan\phi_{12}\,, \end{aligned} \tag{2}$$

where $B(t)$ is the state into which a produced B meson has evolved after a proper time t, and f indicates a flavour-specific final state. The term flavour-specific means that the final state is only reachable by the decay of the B meson, and consequently reachable by a meson originally produced as a $\overline{B}$ only through mixing. We use the semileptonic flavour specific final state and thus refer to this quantity as $a_{\rm sl}$. Note that $a_{\rm sl}$ is decay time independent. In the following discussion, mention of a specific channel implies the inclusion of the charge-conjugate mode, except in reference to $a_{\rm sl}$, the semileptonic B_s^0 *CP* asymmetry.

The phase ϕ_{12}^s is very small in the Standard Model (SM), approximately 0.2° [2].[1] New physics can affect this phase [4, 3] and therefore $a_{\rm sl}^s$. The D0 collaboration has reported evidence for a decay asymmetry $A_{\rm sl}^b = (-0.787 \pm 0.172 \pm 0.093)\%$ in a mixture of B^0 and B_s^0 semileptonic decays, where the first uncertainty is statistical and the second systematic [5]. This asymmetry is much larger in magnitude than the SM predictions for semileptonic asymmetries in $\overline{B}_s^0$ and $\overline{B}^0$ decays, namely $a_{\rm sl}^s = (1.9 \pm 0.3) \times 10^{-5}$ and

[1] This phase should not be confused with the *CP* violation phase measured in $B_s^0 \to J/\psi\,\phi$ and $B_s^0 \to J/\psi\,\pi^+\pi^-$ decays, sometimes called ϕ_s [3].

$a^d_{\rm sl} = (-4.1 \pm 0.6) \times 10^{-4}$ [3]. More recently D0 published measurements of $a^d_{\rm sl} = (0.68 \pm 0.45 \pm 0.14)\%$ [6], and $a^s_{\rm sl} = (-1.12 \pm 0.74 \pm 0.17)\%$ [7], consistent both with the anomalous asymmetry $A^b_{\rm sl}$ and the SM predictions for $a^s_{\rm sl}$ and $a^d_{\rm sl}$. If the measured value of $A^b_{\rm sl}$ is confirmed, this would demonstrate the presence of physics beyond the SM in the quark sector. The e^+e^- B-factory average asymmetry in $\overline{B}^0$ decays is $a^d_{\rm sl} = (0.02 \pm 0.31)\%$ [8], in good agreement with the SM. A measurement of $a^s_{\rm sl}$ with comparable accuracy is important to establish whether physics beyond the Standard Model influences flavour oscillations in the B^0_s system.

When measuring a semileptonic asymmetry at a pp collider, such as the LHC, particle-antiparticle production asymmetries, denoted as $a_{\rm P}$, as well as detector related asymmetries, may bias the measured value of $a^s_{\rm sl}$. We define $a_{\rm P}$ in terms of the numbers of produced b-hadrons, $N(B)$, and anti b-hadrons, $N(\overline{B})$, as

$$a_{\rm P} \equiv \frac{N(B) - N(\overline{B})}{N(B) + N(\overline{B})} \ , \tag{3}$$

where $a_{\rm P}$ may in general be different for different species of b-hadron.

In this paper we report the measurement of the asymmetry between $D^+_s X \mu^- \overline{\nu}$ and $D^-_s X \mu^+ \nu$ decays, with X representing possible associated hadrons. We use the $D^\pm_s \to \phi\pi^\pm$ decay. For a time-integrated measurement we have, to first order in $a^{\rm s}_{\rm sl}$

$$A_{\rm meas} \equiv \frac{\Gamma[D^-_s\mu^+] - \Gamma[D^+_s\mu^-]}{\Gamma[D^-_s\mu^+] + \Gamma[D^+_s\mu^-]} = \frac{a^s_{\rm sl}}{2} + \left[a_{\rm P} - \frac{a^s_{\rm sl}}{2}\right] \frac{\int_{t=0}^{\infty} e^{-\Gamma_s t} \cos(\Delta M_s\, t)\epsilon(t) dt}{\int_{t=0}^{\infty} e^{-\Gamma_s t} \cosh(\frac{\Delta\Gamma_s\, t}{2})\epsilon(t) dt}, \tag{4}$$

where ΔM_s and Γ_s are the mass difference and average decay width of the $B^0_s - \overline{B}^0_s$ meson system, respectively, and $\epsilon(t)$ is the decay time acceptance function for $\overline{B}^0_s$ mesons. Due to the large value of ΔM_s, 17.768 $\pm$0.024 ps^{-1} [9], the oscillations are rapid and the integral ratio in Eq. (4) is approximately 0.2%. Since the production asymmetry within the detector acceptance is expected to be at most a few percent [10, 11, 12], this reduces the effect of $a_{\rm p}$ to the level of a few 10^{-4} for $\overline{B}^0_s$ decays. This is well beneath our target uncertainty of the order of 10^{-3}, and thus can be neglected, therefore yielding $A_{\rm meas}$=0.5 $a^{\rm s}_{\rm sl}$.

The measurement could be affected by a detection charge-asymmetry, which may be induced by the event selection, tracking, and muon selection criteria. The measured asymmetry can be written as

$$A_{\rm meas} = A^{\rm c}_{\mu} - A_{\rm track} - A_{\rm bkg}, \tag{5}$$

where $A_\mu^{\rm c}$ is given by

$$A_\mu^{\rm c} = \frac{N(D_s^-\mu^+) - N(D_s^+\mu^-) \times \frac{\epsilon(\mu^+)}{\epsilon(\mu^-)}}{N(D_s^-\mu^+) + N(D_s^+\mu^-) \times \frac{\epsilon(\mu^+)}{\epsilon(\mu^-)}}. \tag{6}$$

$N(D_s^-\mu^+)$ and $N(D_s^+\mu^-)$ are the measured yields of $D_s\mu$ pairs, $\epsilon(\mu^+)$ and $\epsilon(\mu^-)$ are efficiency corrections accounting for trigger and muon identification effects, $A_{\rm track}$ is the track-reconstruction asymmetry of charged particles, and $A_{\rm bkg}$ accounts for asymmetries induced by backgrounds.

2 The LHCb detector and trigger

We use a data sample corresponding to an integrated luminosity of 1.0 fb^{-1} collected in 7 TeV pp collisions with the LHCb detector [13]. This detector is a single-arm forward spectrometer covering the pseudorapidity range $2 < \eta < 5$, designed for the study of particles containing b or c quarks. The detector includes a high precision tracking system consisting of a silicon-strip vertex detector surrounding the pp interaction region, a large-area silicon-strip detector located upstream of a dipole magnet with a bending power of about 4 Tm, and three stations of silicon-strip detectors and straw drift-tubes placed downstream. The combined tracking system has momentum resolution $\Delta p/p$ that varies from 0.4% at 5 GeV to 0.6% at 100 GeV.[2] Charged hadrons are identified using two ring-imaging Cherenkov (RICH) detectors [14]. Photon, electron and hadron candidates are identified by a calorimeter system consisting of scintillating-pad and pre-shower detectors, an electromagnetic calorimeter and a hadronic calorimeter. Muons are identified by a system composed of alternating layers of iron and multiwire proportional chambers [15]. The LHCb coordinate system is a right handed Cartesian system with the positive z-axis aligned with the beam line and pointing away from the interaction point and the positive x-axis following the ground of the experimental area, and pointing towards the outside of the LHC ring.

The trigger system [16] consists of a hardware stage, based on information from the calorimeter and muon systems, followed by a software stage which applies a full event reconstruction. For the $D_s\mu$ signal samples, the hardware trigger (L0) requires the detection of a muon of either charge with transverse momentum $p_{\rm T} > 1.64$ GeV. In the subsequent software trigger, a first selection algorithm confirms the L0 candidate muon as a fully reconstructed

[2] We work in units with c=1.

track, while the second level algorithm includes two possible selections. One is based on the topology of the candidate muon and one or two additional tracks, requiring them to be detached from the primary interaction vertex. The second category is specifically designed to detect inclusive $\phi \to K^+K^-$ decays. We consider all candidates that satisfy either selection algorithm. We also study two mutually exclusive samples, one composed of candidates that satisfy the second trigger category, and the other satisfying the topological selection of events including a muon, but not the inclusive ϕ algorithm. Approximately 40% of the data were taken with the magnetic field up, oriented along the positive y-axis in the LHCb coordinate system, and the rest with the opposite down polarity. We exploit the fact that certain detection asymmetries cancel if data from different magnet polarities are combined.

3 Selection requirements

Additional selection criteria on muons are that the momentum, p, be between 6 and 100 GeV, that the pseudorapidity, η, be between 2 and 5, and that they are inconsistent with being produced at any primary vertex. Tracks are considered as kaon candidates if they are identified by the RICH system, have $p_{\rm T} > 0.3\,{\rm GeV}$ and $p > 2\,{\rm GeV}$. The impact parameter (IP), defined as the minimum distance of approach of the track with respect to the primary vertex, is used to select tracks coming from charm decays. We require that the χ^2, formed by using the hypothesis that each track's IP is equal to 0, is greater than 9. To be reconstructed as a ϕ meson candidate, a K^+K^- pair must have invariant mass within $\pm 20\,{\rm MeV}$ of the ϕ meson mass. Candidate ϕ mesons are combined with charged pions to make D_s meson candidates. The sum of the $p_{\rm T}$ of K^+, K^- and $\pi^\pm$ candidates must be larger than 2.1 GeV. The vertex fit χ^2 divided by the number of degrees of freedom (ndf) must be less than 6, and the flight distance χ^2, formed by using the hypothesis that the D_s^+ flight distance is equal to 0, must be greater than 100. The B_s^0 candidate, formed from the D_s and the muon, must have vertex fit $\chi^2/{\rm ndf} < 6$, be downstream of the primary vertex, have $2 < \eta < 5$ and have invariant mass between 3.1 and 5.1 GeV. The cosine of the angle between the D_s momentum and the vector from the primary vertex to the D_s decay vertex must be larger than 0.99. In addition, the cosine of the angle between the $D_s\mu$ momentum direction and the vector from the primary vertex to the $D_s\mu$ origin must be larger than 0.999.

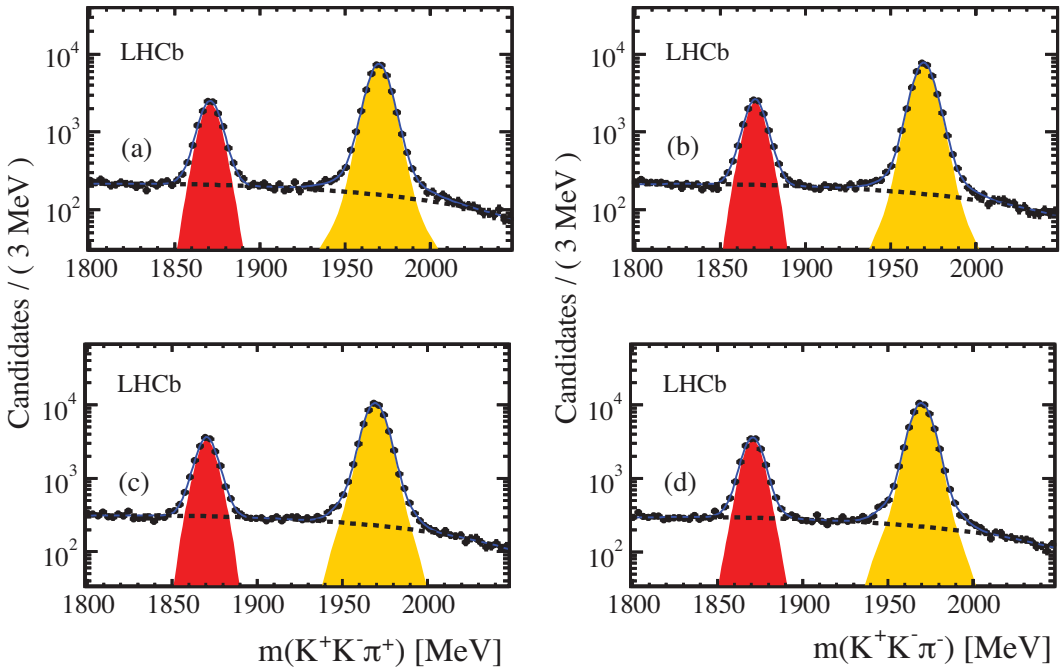

Figure 1: Invariant mass distributions for: (a) $K^+K^-\pi^+$ and (b) $K^+K^-\pi^-$ candidates for magnet up, (c) $K^+K^-\pi^+$ and (d) $K^+K^-\pi^-$ candidates for magnet down with K^+K^- invariant mass within ± 20 MeV of the ϕ meson mass. The D_s^+ [yellow (grey) shaded area] and D^+ [red (dark) shaded area] signal shapes are described in the text.

4 Analysis method

Signal yields are determined by fitting the $K^+K^-\pi^+$ invariant mass distributions shown in Fig. 1. We fit both the signal D_s^+ and D^+ peaks with double Gaussian functions with common means. The D^+ channel is used only as a component of the fit to the mass spectrum. The average mass resolution is about 7.1 MeV. The background is modelled with a second-order Chebychev polynomial. The signal yields from the fits are listed in Table 1.

We use two calibration samples containing muons to measure the relative trigger efficiencies of $D_s^+\mu^-/D_s^-\mu^+$ events, and the relative μ^-/μ^+ identification efficiencies. The first sample contains $b \to J/\psi(\to \mu^+\mu^-)X$ decays triggered independently of the J/ψ meson, and where the J/ψ is selected by requiring two particles of opposite charge have an invariant mass consistent with the J/ψ mass. This sample is called the kinematically-selected (KS) sample. The second sample is collected by triggering on one muon from a J/ψ decay that is detached from the primary vertex. It is called muon

Table 1: Signal B_s^0 yields for $D_s^+\mu^-$ and $D_s^-\mu^+$ events separately for magnet up and down data.

	Magnet up	Magnet down
$D_s^-\mu^+$	$38\,742 \pm 218$	$53\,768 \pm 264$
$D_s^+\mu^-$	$38\,055 \pm 223$	$54\,252 \pm 259$

selected (MS) as it relies on the presence of a well identified muon.

In order to measure the relative π^+ and π^- detection efficiencies, we use the ratio of partially reconstructed and fully reconstructed $D^{*+} \to \pi^+ D^0$, $D^0 \to K^-\pi^+\pi^+(\pi^-)$ decays. The former sample is gathered without explicitly reconstructing the π^- particle, and then the efficiency of finding this track in the event is measured. The same procedure is applied to the charge conjugate mode, so the relative π^+ to π^- efficiency is measured. A detailed description is given in Ref. [17].

Finally, a sample of $D^+(\to K^-\pi^+\pi^+)\mu^-$ candidates is obtained using similar triggers to the $D_s\mu$ sample. This sample is used to assess charge asymmetries induced by the software trigger.

The efficiency ratio $\epsilon_{\mu^+}/\epsilon_{\mu^-}$ in Eq. (6) accounts for losses due to the muon identification efficiency algorithm and the trigger requirements. We measure $\epsilon_{\mu^+}/\epsilon_{\mu^-}$ using the KS and MS calibration samples. There are about 0.6 million KS J/ψ candidates selected in total, and about 1.2 million MS J/ψ candidates. As the calibration muon spectra are slightly softer than that of the signal, we subdivide the signal and calibration samples into subsamples defined by the kinematic properties of the candidate muon. We define five muon momentum bins: $6-20$ GeV, $20-30$ GeV, $30-40$ GeV, $40-50$ GeV, and $50-100$ GeV. We further subdivide the signal and calibration samples with two binning schemes. In the first, each μ momentum bin is split into 10 rectangular regions in qp_x and p_y, where q represents the muon charge and p_x and p_y are the Cartesian components of the muon momentum in the directions perpendicular to the beam axis. The second grid uses 8 regions of muon $p_{\rm T}$ and azimuthal angle ϕ to reduce the sensitivity to differences in ϕ acceptance between signal and calibration samples. In this case the first and third bins in ϕ are flipped for negative charges, to symmetrize the acceptance in a consistent manner with the qp_x and p_y binning. Signal and calibration yields are determined separately in each of the intervals both for magnet up and down data. Figure 2 shows the $\mu^+\mu^-$ invariant mass distribution for the KS J/ψ events in magnet up data.

The relative efficiencies for triggering and identifying muons in five dif-

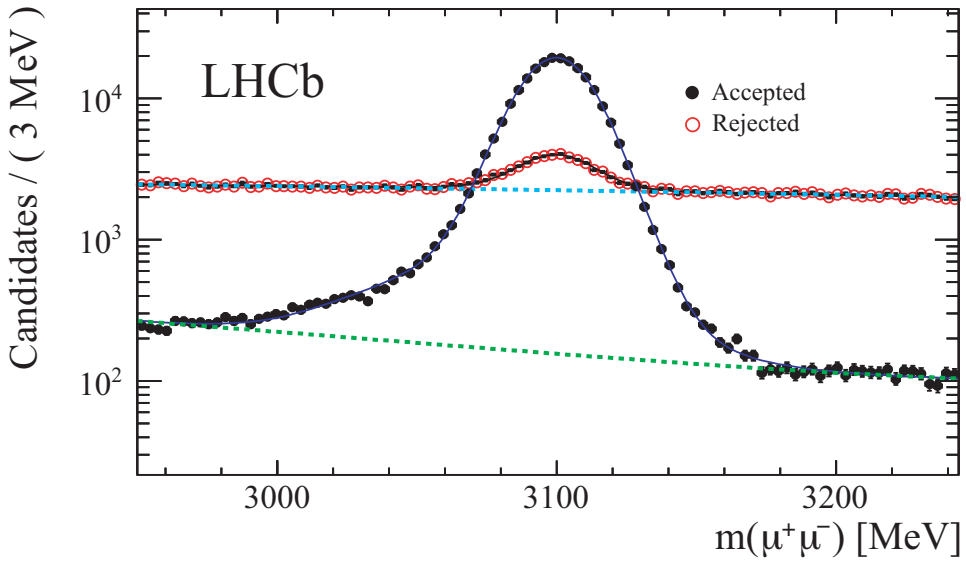

Figure 2: Invariant $\mu^+\mu^-$ mass distributions of the kinematically-selected J/ψ candidates in magnet up data, where the red (open) circles represent entries where the probe candidate is rejected and the black (filled) circles those where the probe is accepted. The dashed lines represent the combinatorial background.

ferent momentum bins are shown in Fig. 3 for magnet up and magnet down data using the KS calibration sample. They are consistent with being independent of momentum. The small difference of approximately 1% between the two samples can be attributed to the alignment of the muon stations, which affects predominantly the hardware muon trigger.

The $D_s^+\mu^-$ final state benefits from several cancellations of potential instrumental asymmetries that can arise due to the different interaction cross-sections in the detector material or to differences between tracking reconstructions of negative and positive particles. The μ and π charged tracks have very similar reconstruction efficiencies. Using the partially-reconstructed D^{*+} calibration sample, we found that the π^+ versus π^- relative tracking efficiencies are independent of momentum and transverse momentum [17]. This, along with the fact that π^+ and π^- interaction cross-sections on isoscalar targets are equal, and that the detector is almost isoscalar, implies that the difference between π^+ and π^- tracking efficiencies depend only upon the magnetic field orientation and the detector acceptance. Thus the charge asymmetry ratios measured for pions are applicable to muons as well. In the $\phi\pi^+\mu^-$ final states, the pion and muon have opposite signs, and thus the charge asymmetry in the track reconstruction efficiency induced by imperfect $\pi\mu$ cancellation, $A^{\pi\mu}_{\rm track}$, is small. Using the efficiency ratios $\epsilon_{\pi^+}/\epsilon_{\pi^-}$ mea-

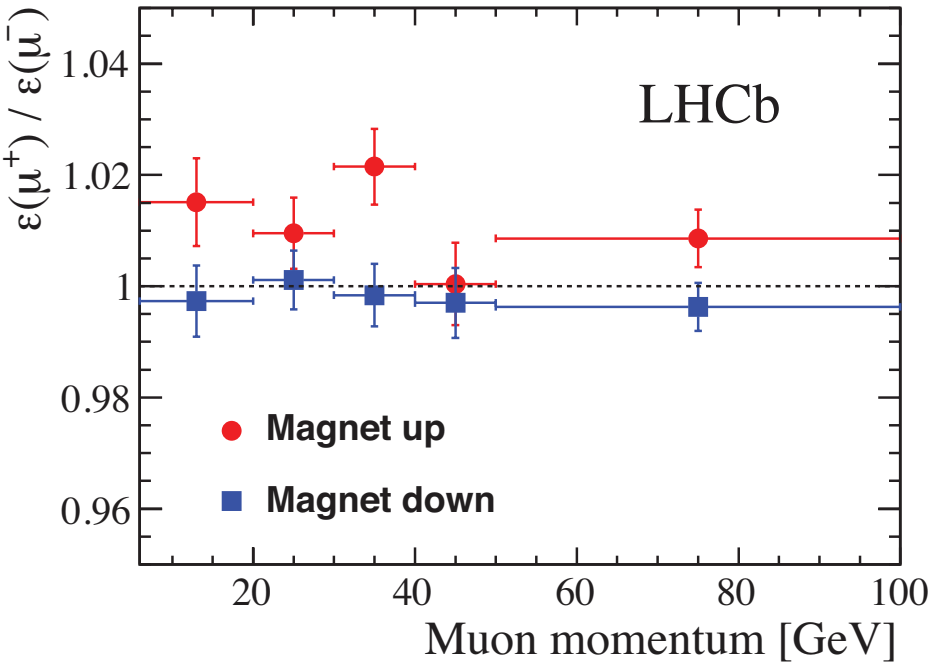

Figure 3: Relative muon efficiency as a function of muon momentum determined using the kinematically-selected J/ψ sample.

sured with the D^{*+} calibration sample, we obtain $A^{\pi\mu}_{\rm track} = (+0.01 \pm 0.13)\%$. A small residual sensitivity to the charge asymmetry in K track reconstruction is present due to a slight momentum mismatch between the two kaons from ϕ decays arising from the interference with the S-wave component. It is determined to be $A^{KK}_{\rm track} = (+0.012 \pm 0.004)\%$. The efficiency ratios used in determining $A^{KK}_{\rm track}$ are based on $\epsilon_{\pi^+}/\epsilon_{\pi^-}$ with a correction derived from the comparison between the Cabibbo-favoured decays $D^+ \to K^-\pi^+\pi^-$ and $D_s^+ \to K^0_S\pi^+$, accounting for additional charge asymmetry induced by K interactions in the detector. Therefore, the total tracking asymmetry is $A_{\rm track} = (+0.02 \pm 0.13)\%$.

5 Backgrounds

Backgrounds include prompt charm production, fake muons associated with real D_s^+ particles produced in b-hadron decays, and $B \to DD_s$ decays where the D hadron decays semileptonically. Here B denotes any meson or baryon containing a b (or $\bar{b}$) quark, and similarly, D denotes any hadron containing

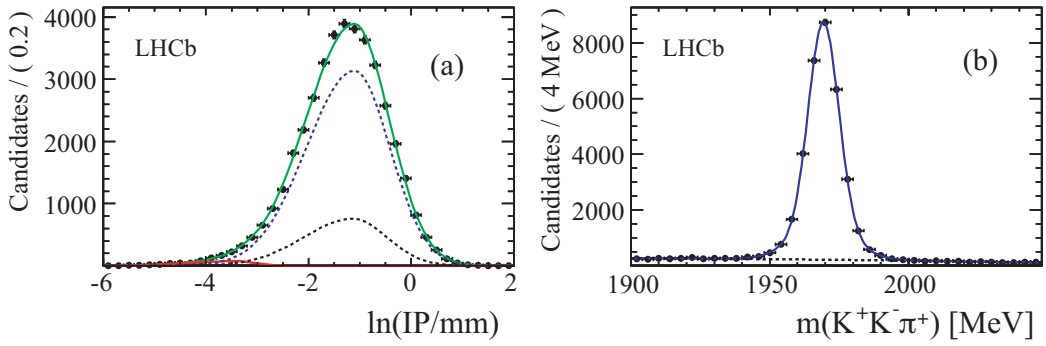

Figure 4: (a) Spectrum of the logarithm of the IP calculated with respect to the primary vertex for D_s^+ candidates in combination with muons. The blue dashed line is the component coming from B hadron decays, the black dashed line the false D_s^+ background, the red line the prompt background, (b) the invariant mass distributions for $D_s^+ \to \phi\pi$ candidates. These distributions are for the magnet down sample.

a c (or $\bar{c}$) quark. The prompt background is highly suppressed by the requirement of a well identified muon forming a vertex with the D_s^+ candidate. The prompt yield is separated from false D_s backgrounds using a binned two-dimensional fit to the mass and ln(IP/mm) of the $\phi\pi^+$ candidates. The method is described in detail in Ref. [18]. Figure 4 shows the fit results for the magnet-down $D_s^+\mu^-$ candidate sample. From the asymmetry in the prompt yield normalized to the overall signal yield in the five momentum bins, we obtain an asymmetry due to prompt background equal to (+0.14±0.07)% for magnet up data, $(-0.05 \pm 0.05)\%$ for magnet down data, with an average value of (+0.04±0.04)%.

Samples of $D_s^+\pi^-X$ and $D_s^+K^-X$ events, where X represents undetected particles from the same decay, are used to infer the numbers of D_s^+-hadron combinations from B decays that could be mistaken for $D_s^+\mu^-$ events if the hadron is misidentified as a muon. Kaons and pions are identified using the RICH. These numbers, combined with knowledge of the probability that kaons or pions are mistaken for muons, provide a measurement of the fake hadron background. These misidentification probabilities are also calculated in the five momentum bins using $D^{*+} \to \pi^+ D^0$ decays, with D^0 decaying into the $K^-\pi^+$ final state. The net effect on the asymmetry is below 10^{-4} and thus the D_s^+-hadron background can be ignored.

We also consider the background induced by $D_s^+\mu^-$ events deriving from $b \to c\bar{c}s$ decays where the D_s^+ hadron originates from the virtual W^+ boson and the muon originates from the charmed-hadron semileptonic decay.

These backgrounds are suppressed since the D hadron travels away from the B vertex prior to its semileptonic decay. As these decays are of opposite sign to the signal, they cause a background asymmetry that is proportional to the production asymmetry of the background sources. The B^0 production asymmetry has been measured in LHCb to be $(-0.1 \pm 1.0)\%$ [11], and the B^+ production asymmetry to be $(+0.3 \pm 0.9)\%$ by comparing $B^+ \to J/\psi K^+$ and $B^- \to J/\psi K^-$ decays [19]. A small subset of this background is from Λ_b^0 decays, whose production asymmetry is not well known, $a_{\rm P} = (-1.0 \pm 4.0)\%$, but is consistent with zero [20]. The $\overline{B}^0$ final states include $\overline{D}^0$ and D^- hadrons, in proportions determined according to the D^{*+}/D^+ ratio in the measured exclusive final states. In addition, we consider backgrounds coming from $B^0, B^+ \to D_s^- K \mu^+$ decays, that provide a background asymmetry with opposite sign. We estimate this background asymmetry to be $(+0.01 \pm 0.04)\%$. The systematic uncertainty includes the limited knowledge of the inclusive branching fraction of the b-hadrons, uncertainties in the b-hadron production ratios, and in the charm semileptonic branching fractions, but is dominated by the uncertainty in the production asymmetry. By combining these estimates, we obtain $A_{\rm bkg} = (+0.05 \pm 0.05)\%$.

6 Results

We perform weighted averages of the corrected asymmetries A_μ^c observed in each $p_{\rm T}\phi$ and $p_x p_y$ subsample, using muon identification corrections both in the KS and MS sample. The results are shown in Table 2. The agreement between the four results obtained with different combinations of kinematic binning and muon calibration methods is good. The corrected asymmetries in each of the muon momentum bins are shown in Fig. 5. The data points are consistent with having no dependence upon muon momentum; for example the data points shown in Fig. 5(e) and (f) are consistent with this hypothesis with a p-value of 1.7% and 2.9%, respectively. Possible sources of systematic uncertainties are described below.

In order to obtain the final results, we perform an arithmetic average of the four values of A_μ^c obtained with the two binning schemes chosen and with the two muon correction methods, assuming the results to be fully statistically correlated, and obtain $A_\mu^c = (+0.04 \pm 0.25)\%$. We then correct for tracking efficiency asymmetries and background asymmetries, and obtain

$$A_{\rm meas} = (-0.03 \pm 0.25 \pm 0.18)\%,$$

where the first uncertainty reflects statistical fluctuations in the signal yield

Table 2: Muon efficiency ratio corrected asymmetry A_μ^c. The errors account for the statistical uncertainties in the B_s^0 signal yields.

A_μ^c [%]	KS muon correction		MS muon correction		Average
Magnet	$p_x p_y$	$p_{\rm T}\phi$	$p_x p_y$	$p_{\rm T}\phi$	
Up	$+0.38 \pm 0.38$	$+0.30 \pm 0.38$	$+0.64 \pm 0.37$	$+0.63 \pm 0.37$	$+0.49 \pm 0.38$
Down	-0.17 ± 0.32	-0.25 ± 0.32	-0.60 ± 0.32	-0.62 ± 0.32	-0.41 ± 0.32
Avg.	$+0.11 \pm 0.25$	$+0.02 \pm 0.25$	$+0.02 \pm 0.24$	$+0.01 \pm 0.24$	$+0.04 \pm 0.25$

and the second reflects the systematic uncertainties. This gives

$$a_{\rm sl}^s = (-0.06 \pm 0.50 \pm 0.36)\%.$$

We consider several sources of systematic uncertainties on $A_{\rm meas}$ that are summarized in Table 3. By examining the variations on the average A_μ^c obtained with different procedures, we assign a 0.07% uncertainty, reflecting three almost equal components: the fitting procedure, the kinematic binning and a residual systematic uncertainty related to the muon efficiency ratio calculation. We study the effect of the fitting procedure by comparing results obtained with different models for signal and background shapes. In addition, we consider the effects of the statistical uncertainties of the efficiency ratios, assigning 0.08%, which is obtained by propagating the uncertainties in the average A_μ^c. The uncertainties affecting the background estimates are discussed in Sec. 5. Possible changes in detector acceptance during magnet up and magnet down data taking periods are estimated to contribute 0.01%. The software trigger systematic uncertainty is mainly due to the topological trigger algorithm and is estimated to be 0.05%. These uncertainties are considered uncorrelated and added in quadrature to obtain the total systematic uncertainty.

Table 3: Sources of systematic uncertainty on A_{meas}.

Source	$\sigma(A_{\text{meas}})[\%]$
Signal modelling and muon correction	0.07
Statistical uncertainty on the efficiency ratios	0.08
Background asymmetry	0.05
Asymmetry in track reconstruction	0.13
Field-up and field-down run conditions	0.01
Software trigger bias (topological trigger)	0.05
Total	0.18

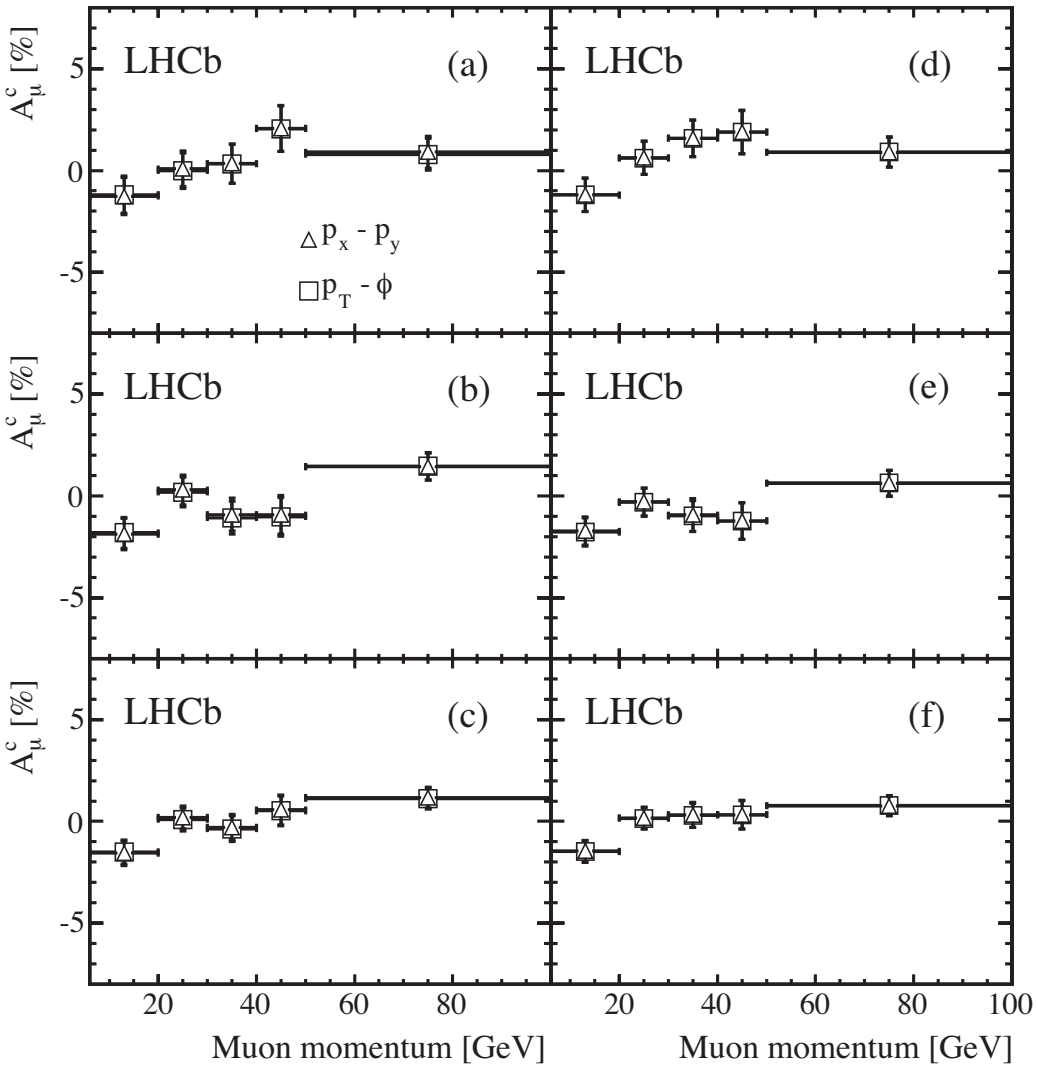

Figure 5: Asymmetries corrected for relative muon efficiencies, A_μ^c, examined in the five muon momentum intervals for (a) magnet up data, (b) magnet down data and (c) average, using the KS muon calibration method. Then (d) magnet up data, (e) magnet down data and (f) average, using the MS muon calibration method in the two different binning scheme.

7 Conclusions

We measure the asymmetry $a^s_{\rm sl}$, which is twice the measured asymmetry between $D_s^-\mu^+$ and $D_s^+\mu^-$ yields, to be

$$a^s_{\rm sl} = (-0.06 \pm 0.50 \pm 0.36)\%.$$

Figure 6 shows this measurement, the D0 measured asymmetries in dimuon decays in 1.96 TeV $p\overline{p}$ collisions of $A^b_{\rm sl} = (-0.787 \pm 0.172 \pm 0.093)\%$ [5], $a^d_{\rm sl} = (0.68 \pm 0.45 \pm 0.14)\%$ [6], and $a^s_{\rm sl} = (-1.12 \pm 0.74 \pm 0.17)\%$ [7], and the most recent average from B-factories [8], namely $a^d_{\rm sl} = (0.02 \pm 0.31)\%$. Our result for $a^s_{\rm sl}$ is currently the most precise measurement made and is consistent with the Standard Model.

Acknowledgements

We express our gratitude to our colleagues in the CERN accelerator departments for the excellent performance of the LHC. We thank the technical and administrative staff at the LHCb institutes. We acknowledge support from CERN and from the national agencies: CAPES, CNPq, FAPERJ and FINEP (Brazil); NSFC (China); CNRS/IN2P3 and Region Auvergne (France); BMBF, DFG, HGF and MPG (Germany); SFI (Ireland); INFN (Italy); FOM and NWO (The Netherlands); SCSR (Poland); MEN/IFA (Romania); MinES, Rosatom, RFBR and NRC "Kurchatov Institute" (Russia); MinECo, XuntaGal and GENCAT (Spain); SNSF and SER (Switzerland); NAS Ukraine (Ukraine); STFC (United Kingdom); NSF (USA). We also acknowledge the support received from the ERC under FP7. The Tier1 computing centres are supported by IN2P3 (France), KIT and BMBF (Germany), INFN (Italy), NWO and SURF (The Netherlands), PIC (Spain), GridPP (United Kingdom). We are thankful for the computing resources put at our disposal by Yandex LLC (Russia), as well as to the communities behind the multiple open source software packages that we depend on.

References

[1] U. Nierste, *Three lectures on meson mixing and CKM phenomenology*, arXiv:0904.1869.

[2] A. Lenz and U. Nierste, *Theoretical update of $B^0_s - \overline{B}^0_s$ mixing*, JHEP **06** (2007) 072, arXiv:hep-ph/0612167.

[3] A. Lenz, *Theoretical update of B-mixing and lifetimes*, arXiv:1205.1444.

[4] C. Bobeth and U. Haisch, *New Physics in* Γ_{12}^s*:* $(\bar{s}b)(\bar{\tau}\tau)$ *operators*, Acta Phys. Polon. **B44** (2013) 127, arXiv:1109.1826.

[5] D0 collaboration, V. M. Abazov *et al.*, *Measurement of the anomalous like-sign dimuon charge asymmetry with 9* fb^{-1} *of* $p\bar{p}$ *collisions*, Phys. Rev. **D84** (2011) 052007, arXiv:1106.6308; D0 collaboration, V. M. Abazov *et al.*, *Evidence for an anomalous like-sign dimuon charge asymmetry*, Phys. Rev. **D82** (2010) 032001, arXiv:1005.2757; D0 collaboration, V. M. Abazov *et al.*, *Evidence for an anomalous like-sign dimuon charge asymmetry*, Phys. Rev. Lett. **105** (2010) 081801, arXiv:1007.0395.

[6] D0 collaboration, V. M. Abazov *et al.*, *Measurement of the semileptonic charge asymmetry in* B^0 *meson mixing with the D0 detector*, Phys. Rev. **D86** (2012) 072009, arXiv:1208.5813.

[7] D0 collaboration, V. M. Abazov *et al.*, *Measurement of the semileptonic charge asymmetry using* $B_s^0 \to D_s \mu X$ *decays*, Phys. Rev. Lett. **110** (2013) 011801, arXiv:1207.1769.

[8] Heavy Flavor Averaging Group, D. Asner *et al.*, *Averages of b-hadron, c-hadron, and* τ*-lepton properties*, arXiv:1010.1589, online updates available at http://www.slac.stanford.edu/xorg/hfag/.

[9] LHCb collaboration, R. Aaij *et al.*, *Precision measurement of the* B_s^0-$\bar{B}_s^0$ *oscillation frequency with the decay* $B_s^0 \to D_s^- \pi^+$, New J. Phys. **15** (2013) 053021, arXiv:1304.4741.

[10] E. Norrbin and R. Vogt, *Bottom production asymmetries at the LHC*, arXiv:hep-ph/0003056, in proceedings of the CERN 1999 Workshop on SM physics (and more) at the LHC.

[11] LHCb collaboration, R. Aaij *et al.*, *First observation of CP violation in the decays of* B_s^0 *mesons*, Phys. Rev. Lett. **110** (2013) 221601, arXiv:1304.6173.

[12] LHCb collaboration, R. Aaij *et al.*, *Measurements of the branching fractions and CP asymmetries of* $B^+ \to J/\psi\pi^+$ *and* $B^+ \to \psi(2S)\pi^+$ *decays*, Phys. Rev. **D85** (2012) 091105, arXiv:1203.3592.

[13] LHCb collaboration, A. A. Alves Jr. *et al.*, *The LHCb detector at the LHC*, JINST **3** (2008) S08005.

[14] M. Adinolfi *et al.*, *Performance of the LHCb RICH detector at the LHC*, Eur. Phys. J. **C73** (2013) 2431, arXiv:1211.6759.

[15] A. A. Alves Jr *et al.*, *Performance of the LHCb muon system*, JINST **8** (2013) P02022, arXiv:1211.1346.

[16] R. Aaij *et al.*, *The LHCb trigger and its performance in 2011*, JINST **8** (2013) P04022, arXiv:1211.3055.

[17] LHCb collaboration, R. Aaij *et al.*, *Measurement of the $D_s^+ - D_s^-$ production asymmetry in 7 TeV pp collisions*, Phys. Lett. **B713** (2012) 186, arXiv:1205.0897.

[18] LHCb collaboration, R. Aaij *et al.*, *Measurement of b-hadron production fractions in 7 TeV pp collisions*, Phys. Rev. **D85** (2012) 032008, arXiv:1111.2357.

[19] LHCb collaboration, R. Aaij *et al.*, *Measurements of the branching fractions and CP asymmetries of $B^+ \to J/\psi\,\pi^+$ and $B^+ \to \psi(2S)\pi^+$ decays*, Phys. Rev. **D85** (2012) 091105, arXiv:1203.3592.

[20] CMS collaboration, S. Chatrchyan *et al.*, *Measurement of the Λ_b cross section and the $\overline{\Lambda}_b$ to Λ_b ratio with $J/\psi\ \Lambda$ decays in pp collisions at $\sqrt{s} = 7$ TeV*, Phys. Lett. **B714** (2012) 136, arXiv:1205.0594.

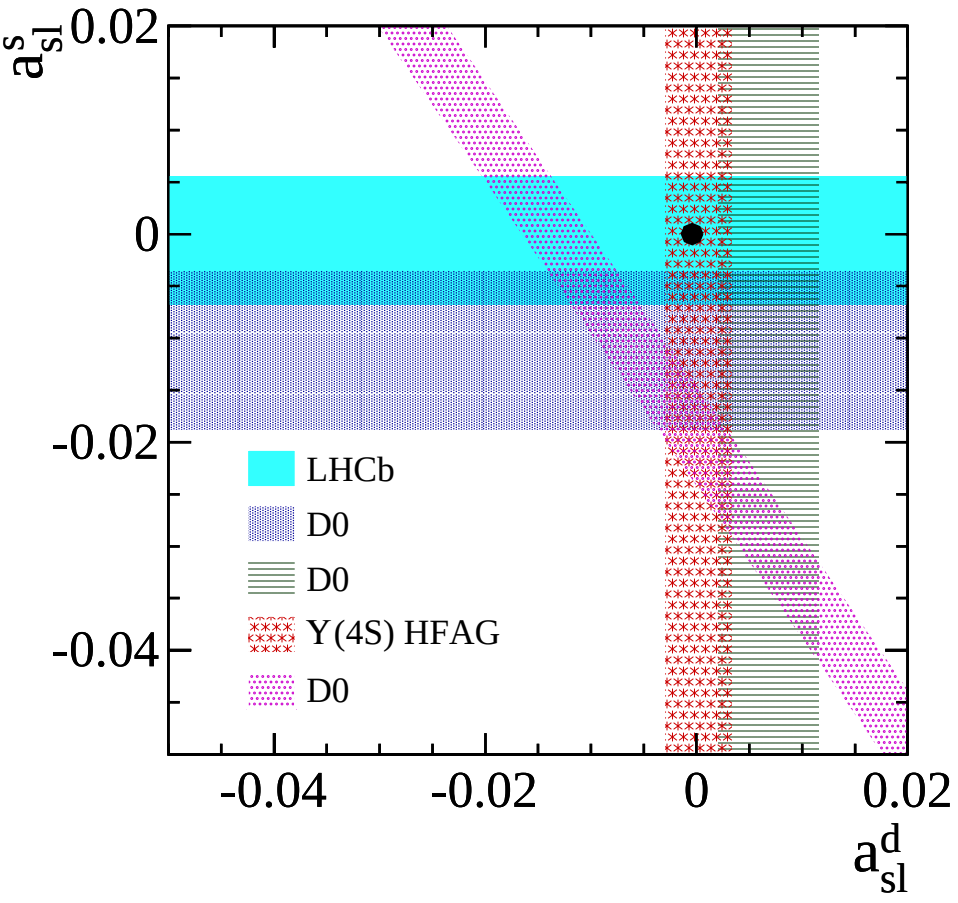

Figure 6: Measurements of semileptonic decay asymmetries. The bands correspond to the central values ± 1 standard deviation uncertainties, defined as the sum in quadrature of the statistical and systematic errors. The point indicates the SM prediction.